

Preparation and Characterization of Poly(chlorotrifluoroethylene-co-ethylvinyl ether)/Poly(styrene acrylate) Core–Shells and SiO₂ Nanocomposite Films via a Solution Mixing Method

C. Koti Reddy, T. Shekharam, D. Shailaja

Polymer Functional Materials Division, Indian Institute of Chemical Technology, Hyderabad 500 607, India

Received 21 November 2011; accepted 8 January 2012

DOI 10.1002/app.36777

Published online in Wiley Online Library (wileyonlinelibrary.com).

ABSTRACT: Nanocomposite particles of poly(chlorotrifluoroethylene-co-ethylvinyl ether) [poly(CTFE-co-EVE)]/poly(styrene acrylate) (PSA)/SiO₂ were prepared with poly(CTFE-co-EVE)/PSA [CS(FS); core-shell (CS) fluoro surfactant (FS)] and hydrophilic SiO₂ nanoparticles by a solution mixing method. This method yielded a homogeneous dispersion of hydrophilic SiO₂ nanoparticles in the CS(FS) matrix. The nanocomposite particle composition was confirmed by Fourier transform infrared spectroscopy and thermogravimetric analysis. A slight improvement in the thermal stability was observed and the glass-transition temperature of the nanocomposite particles increased compared

with the CS(FS) matrix. A remarkable enhancement was observed in the mechanical properties with an increase in the tensile strength from 1.1 to 6.2 MPa and with an increase in the elongation at break from 209.6 to 350.1% for the films with 15 wt % SiO₂. The presence of a wettable PSA shell on the fluorocore made interaction possible with SiO₂; this made it more hygroscopic with a decent water uptake capacity and an enhanced water contact angle. © 2012 Wiley Periodicals, Inc. *J. Appl. Polym. Sci.* 000: 000–000, 2012

Key words: coatings; curing of polymers; resins; stress; thermosets

INTRODUCTION

Organic–inorganic nanocomposites with well-defined structures and morphologies are a very interesting class of materials because of their potential use in a wide range of applications, such as in the automobile, household, and electrical industries.^{1,2} These nanocomposites not only can provide improvement in traditional physical properties, such as mechanical, thermal, and chemical resistance, but also exhibit unique optical, electrical, and magnetic properties.^{3–10} Particularly, silica-based hybrid materials with well-defined morphologies are a promising class of materials that find potential uses in many fields, including plastics, rubbers, and coatings.^{11–13} The ideal properties of polymer/silica nanocomposites should be strongly dependent on the uniform dispersal of nanosilica in the polymer matrix because silica has the tendency to form aggregates if it is not surface-modified.

Of the various approaches for the formation of nanocomposites, the commonly preferred one is via a sol–gel process by *in situ* emulsion

polymerization.^{14,15} Inorganic particles are mostly premodified by a coupling agent to obtain uniform and homogeneously dispersed composites and exhibit good flow properties.^{16–18} Zhang et al.¹⁹ prepared poly(methacrylic methacrylate) (PMMA)/silica hybrid materials via a sol–gel process; these materials displayed a high transparency and heat stability. Bokobza et al.²⁰ reported that silica sol modified by silane coupling agents was mixed with acrylate monomers to obtain silica-based hybrid films by ultraviolet radiation. Chang et al.²¹ prepared PMMA/silica nanocomposites via the *in situ* polycondensation of alkoxysilane in the presence of trialkoxysilane-functional PMMA. Xia et al.²² used an ultrasonically induced encapsulating emulsion polymerization technique to prepare polymer/inorganic nanocomposites. Other options, such as melt mixing and solution mixing of both organic and inorganic components, are the most convenient and economical ways of obtaining hybrid materials but have received only limited successful results. This is mainly due to the agglomeration of inorganic nanoparticles during blending.^{23,24} However, the solution mixing of each component in a cosolvent can help overcome the problem of agglomeration because of the possibility of molecular-level mixing and can be applicable for polymers that can be swollen or dissolved in a solvent.²⁵ To get a perfect blend, the

Correspondence to: D. Shailaja (sdonempudi@iict.res.in).

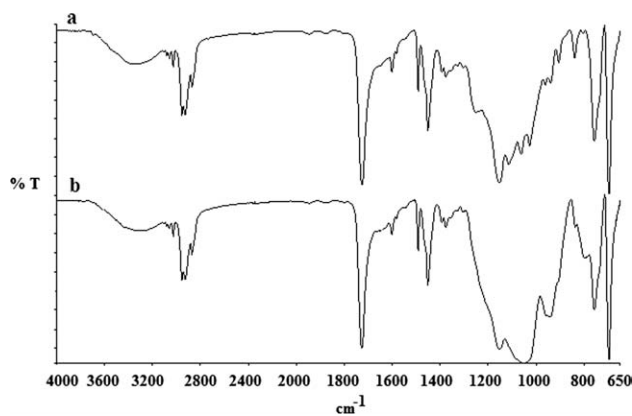


Figure 1 FTIR spectra of (a) CS(FS) and (b) the 20% silica composite.

nanoparticle size, size distribution, aspect ratio, degree of dispersion and orientation, and adhesion at the inorganic–organic interface becomes very important.^{26–28} Kim and Chae²⁹ reported the preparation of PS and hydrophilic ZnO nanocomposites by solution mixing, although both phases had very little compatibility with each other. Cosolvents are known to bring forth better dissolution for some polymers and, sometimes, even faster dissolution rates. This is ascribed to the fact that the cosolvent has the power to break the nanoparticle agglomerate apart and to prevent reagglomeration during solution mixing and film casting.

Nanocomposites of silica with fluoropolymer are known for their practical importance in protective coatings because of their extraordinary properties, such as ultralow surface tension and related hydrophobicity, good chemical and thermal stability, low flammability and low refractive index, and excellent mechanical behavior in protective coatings. In a recent communication,³⁰ we reported the synthesis

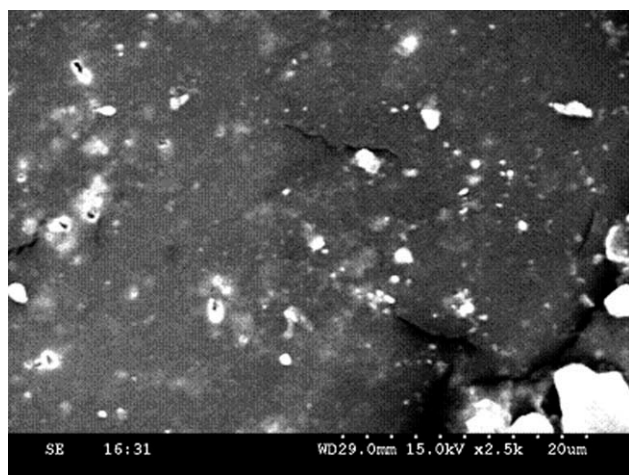


Figure 2 SEM image of the CS(FS) 15% silica nanocomposite.

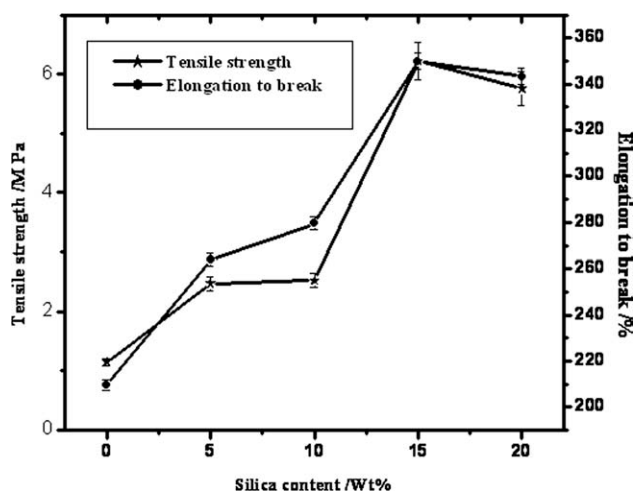


Figure 3 Mechanical properties of CS(FS) and its silica nanocomposite films.

of a film-forming core–shell (CS) emulsion with poly(chlorotrifluoroethylene-*co*-ethylvinyl ether) as the core and poly(styrene acrylate) as the shell. Here, the surface of the hydrophobic fluoropolymer was modified by the encapsulation of a shell polymer that rendered compatibility and is henceforth called the core–shell fluoro surfactant [CS(FS)]. In this study, we adopted the solution mixing method with a cosolvent to make nanocomposites of the this CS emulsion with hydrophilic silica. This modification was anticipated to enable the CS-modified fluoropolymer to form a nanoscale dispersion with hydrophilic silica nanoparticles. The aim of this study was to show how efficiently the mechanical performance of the nanocomposites and their wetting and thermal properties could be improved with this approach.

EXPERIMENTAL

Materials

Silicon dioxide was purchased from Aldrich and consisted of particles with a spherical shape, an average diameter of 10 nm, and a narrow size distribution. Chloroform was purchased from SD Fine Chemicals (Mumbai, India). The preparation of sample CS(FS) (where FS is heptadecafluorooctane sulfonic acid potassium salt) was previously reported.³⁰

Preparation of the CS(FS)/SiO₂ nanocomposites

The CS(FS) compound as the matrix was dissolved in chloroform completely before SiO₂ particles were introduced and dispersed in the solution with constant stirring. The mass fractions of SiO₂ in the composites were varied from 0 to 20%. After 24 h of stirring, thin films were obtained by solution

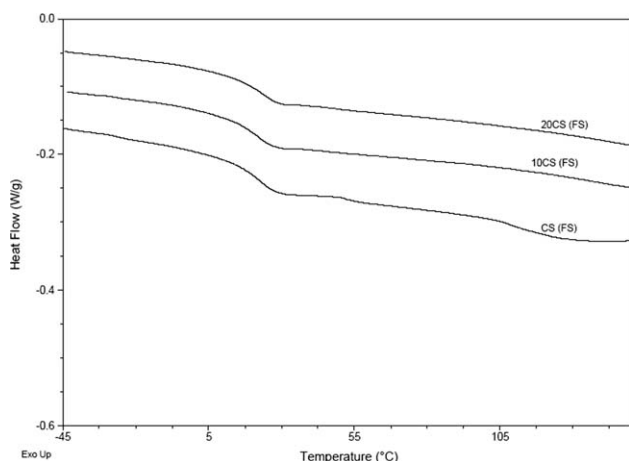


Figure 4 DSC thermograms of CS(FS) and its nanocomposite film.

casting. The mixture of CS(FS) and SiO₂ powders were cast onto a glass slide, and then, the chloroform was vaporized at room temperature, and the film was left to dry for 4 h *in vacuo* at 50°C. The thickness of the films was maintained between 30 and 50 μm.

Characterization of the nanocomposites

The solid content of the latex dispersion was determined gravimetrically. The confirmation of the presence of functional groups was done with Fourier transform infrared (FTIR) spectroscopy recorded on a Thermo Nicolet Nexus 670 spectrometer (Massachusetts, USA). Thermogravimetric analysis (TGA) was performed with a TA Instruments TGA Q500 Universal at a heating rate of 10°C/min under a nitrogen atmosphere. Differential scanning calorimetry (DSC) analysis of the samples was performed on a DSC Q 100 Universal instrument (New Castle, USA). Samples were run in aluminum pans and scanned at a heating rate of 10°C/min under an N₂ atmosphere. Static contact angles were measured on a contact angle goniometer (Kruss GMBH German G10MK2) by the sessile drop method at 25°C. Deionized water was dropped with a microsyringe onto the surface of the latex films. The average value of the angles

TABLE I
TGA Details of CS(FS) and Its Nanocomposite Particles

Sample code	Degradation temperature	Final residue of silica (wt %)
CS(FS)	387	—
5CS(FS)	397	5.8
10CS(FS)	397	9.7
15CS(FS)	395	12.5
20CS(FS)	395	14.3

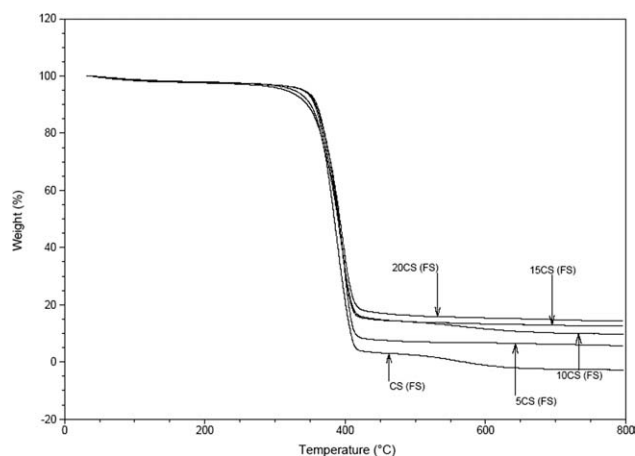


Figure 5 TGA thermograms of CS(FS) and its nanocomposite film.

obtained at more than 10 different locations on each sample surface is reported. The static immersion test is considered as a standard method for evaluating the water resistance of films with the gravimetric method. Samples of films with dimensions of 2 cm × 2 cm × 0.15 mm were immersed in distilled water at 25°C. At specific time intervals, the samples were removed and weighed after they were blotted with a piece of paper towel to absorb excess water on the surfaces. The tensile properties of the films were measured by a universal testing machine (AGS-10k NG; Shimadzu, Japan). The test specimens were in the form of dumbbells according to ASTM D 638. The gauge length was 50 mm, and the crosshead speed was 10 mm/min. The data reported are the average of five measurements.

RESULTS AND DISCUSSION

Structural and morphological properties

Figure 1 shows the FTIR spectra of CS(FS) and its nanocomposite particles of silica. The FTIR spectrum of CS(FS) displayed characteristic absorption peaks at 3435 cm⁻¹ (O—H stretching mode), 2971 and 2929 cm⁻¹ (C—H stretching modes), 1730 cm⁻¹ (—C=O stretching mode), 1458 and 1376 cm⁻¹ (C—H bending modes), 1216, 1122, and 1063 cm⁻¹ (C—O—C stretching modes), CF group stretching, CF₂ groups (C—F asymmetric stretching mode), and (C—F symmetric stretching mode) in the region between 1222 and 1130 cm⁻¹ and at lower wave numbers of 759 cm⁻¹ (C—Cl stretching mode).³⁰ When silica was added to the CS(FS) matrix, no distinct change was observed between the FTIR spectra of CS(FS) and its silica composite except for a strong absorption peak at 1064 cm⁻¹; this may have been affected by the minimal formation of Si—O—Si groups in the composite states. The film of 15% SiO₂ showed a

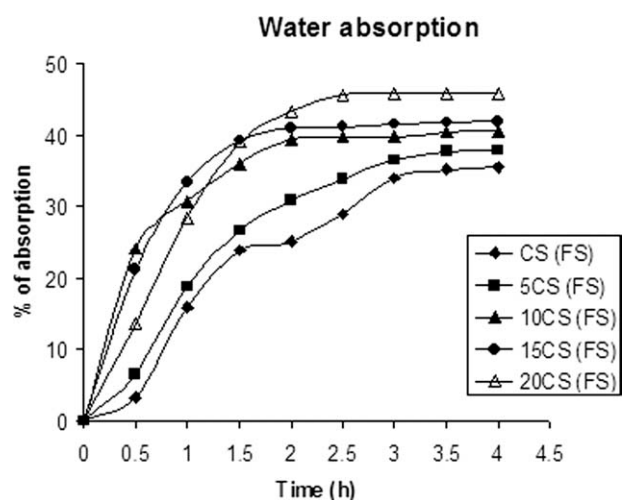


Figure 6 Water absorbance of CS(FS) and its nanocomposite films.

uniform and homogeneous distribution of silica nanoparticles, as shown in Figure 2.

Mechanical properties

Figure 3 shows the relationship of the mechanical properties and the silica filling content of the CS(FS) nanocomposites. Both the tensile strength and elongation at break increased with increasing filling content up to 15 wt %; this was followed by a reduction at higher SiO₂ contents. The CS(FS) nanocomposite filled with 15 wt % hybrids showed not only an adhesive interface but also a remarkable enhancement in the mechanical properties. Its tensile strength increased from 1.1 to 6.2 M Pa, and the elongation at break increased from 209.6 to 350.1% in comparison with that of the unfilled CS(FS) film.¹⁵ At 15%, the dispersion of silica nanoparticles in the polymer matrix probably was at its optimum; when the silica content was increased further, this was not found because a decrease in the tensile properties was noticed.

Glass-transition temperature (T_g)

Figure 4 shows the DSC curves of CS(FS) and its silica filled nanocomposite films. The T_g values for CS(FS) and the 10 and 20 wt % CS(FS)–silica hybrids were measured to be 21.3, 21.9, and 24.1°C, respectively, and are shown in Figure 3. It is obvious that T_g increased with hybrid filling; this suggested that inorganic particles played a role in inhibiting the polymer segmental motion. According to Eisenberg's model, the interaction of polymer chains with nanosilica reduces the mobility of polymer chains and leads to the formation of immobilized and restricted mobility regions around the filler particles. The DSC

spectra clearly indicated restricted segmental motion and polymer–hybrid interactions.

Thermal stability of the latex films

The thermal decomposition behavior of the CS(FS) sample with different silica contents was investigated by TGA at a heating rate of 10°C/min under a nitrogen flow, as illustrated in Figure 5, which reveals single principal thermal event occurring in the following temperature zone: room temperature to 800°C. Obviously, we observed an increase of about 5–10°C from the initial decomposition temperature as silica was incorporated into CS(FS). This also verified the successful incorporation of silica into the nanocomposite particles. Furthermore, the silica contents of the CS(FS) samples were determined from the weight loss of the samples at 800°C. The final residual weight of silica in the CS(FS) nanocomposite particles is listed in Table I.

Water sorption capacities

The water absorption values of CS(FS) and its composite films are shown in Figure 6. From the figure, it can be observed that the water absorption increased with increasing filling silica content. The water absorption of the CS(FS) film was about $35.5 \pm 0.4\%$, whereas the water absorptions of the CS(FS) nanocomposite films filled with 5, 10, 15, and 20 wt % hybrids became 37.9 ± 0.3 , 40.4 ± 0.2 , 41.9 ± 0.4 , and $45.8 \pm 0.1\%$, respectively. Our results demonstrated obvious water-surrender characteristics in the CS(FS) composite film, maybe due to the formation of hydrophilic linkages between silicon dioxide and the acrylic shell of the CS(FS) structure.

Wettability

The contact angles of CS(FS) and its nanocomposite latex film with various silicon dioxide contents are shown in Table II. The contact angle of the CS(FS) films (62°) decreased with increasing silicon dioxide content. The decreasing water contact, because of the hydrophilic nature of silicon dioxide, interacted with the CS(FS) structure.

TABLE II
Water Contact Angles of CS(FS) and Its Nanocomposite Films

Sample code	Water contact angle (°)
CS(FS)	62
5CS(FS)	52
10CS(FS)	50
15CS(FS)	47
20CS(FS)	47

CONCLUSIONS

It was possible to make homogeneously dispersed CS(FS)/SiO₂ nanocomposite particles by solution mixing with hydrophilic SiO₂ in the CS(FS) matrix. This was ascribed to the fact that the cosolvent had the power to break the nanoparticle agglomerate apart and prevent reagglomeration during solution mixing and film casting. The introduction of SiO₂ nanoparticles increased the T_g value slightly and improved the thermal stability. The presence of SiO₂ nanoparticles made little change to the IR spectrum; this was indicative of minimum compatibility between CS(FS) and SiO₂. The hydrophilicity increased with increasing SiO₂ content in the CS(FS) matrix. The introduction of SiO₂ nanoparticles into CS(FS) resulted in excellent tensile properties. This implied that the interfacial adhesion was strong enough to stand large mechanical forces.

References

1. Nylon Plastics; Kohan, M. I., Ed.; Wiley: New York, 1973.
2. Yang, F.; Ou, Y.; Yu, Z. *J Appl Polym Sci* 1998, 69, 355.
3. Philipp, G.; Schmidt, H. *J. Non Cryst Solids* 1984, 63, 283.
4. Morikawa, A.; Iyoku, Y.; Kakimoto, M.; Imai, Y. *Polym J* 1992, 24, 107.
5. Novak, B. M.; Ellsworth, M. W.; Verrier, C. *Polym Mater Sci Eng* 1993, 70, 266.
6. Schmidt, H.; Wolter, N. H. *Non-Cryst Solids* 1990, 121, 428.
7. Popall, M.; Meyer, H.; Schmidt, H.; Schulz, J. *Mater Res Soc Symp Proc* 1990, 180, 995.
8. Glaser, R. H.; Wilkes, G. L. *Polym Bull* 1989, 19, 51.
9. Pope, E. J. A.; Mackenzie, J. D. *MRS Bull* 1987, 12, 29.
10. Pope, E. J. A.; Asami, A.; Mackenzie, J. D. *J Mater Res* 1989, 4, 1018.
11. Kasiwagi, T.; Morgan, A. B.; Antonucci, J. M.; VanLandingham, M. R.; Harris, R. H., Jr.; Awad, W. H.; Shields, J. R. *J Appl Polym Sci* 2003, 89, 2072.
12. Peng, Z.; Kong, L. X.; Li, S. D.; Chen, Y.; Huang M. F. *Compos Sci Technol* 2007, 67, 3130.
13. Mammeri, F.; Rozes, L.; Bourhis, E. L.; Sanchez, C. *J Eur Ceram Soc* 2006, 26, 267.
14. Ma, J. D.; Hu, J.; Zhang, Z. *J. Eur Polym J* 2007, 43, 4169.
15. Aiping, Z.; Aiyun, C.; Ziyi, Y.; Weidong, Z. *J Colloid Interface Sci* 2008, 322, 51.
16. Kiss, G. *Polym Eng Sci* 1987, 27, 410.
17. Thomason, J. L. In *Interfaces in Polymer, Ceramic, and Metal Matrix Composites*; Ishida, H., Ed.; Elsevier: New York, 1988.
18. Ishida, H. *Polym Compos* 1984, 5, 101.
19. Zhang, Q. W.; Zhang, Y. H.; Chen, S. M. *Appl Chem* 2002, 19, 874.
20. Bokobza, L.; Gamaud, G.; Mark, J. E. *Chem Mater* 2002, 14, 162.
21. Chang, T. C.; Wang, Y. T.; Hong, Y. S.; Chiu, Y. S. *J Polym Sci Part B: Polym Chem* 2000, 38, 1972.
22. Xia, H.; Zhang, C.; Wang, Q. *J Appl Polym Sci* 2001, 80, 1130.
23. Alexandre, M.; Dubois, P. *Mater Sci Eng* 2000, 28, 1.
24. Ou, Y.; Yang, F.; Zhuang, Y. *Acta Polym Sci* 1997, 2, 199.
25. Nalwa, H. S. *Handbook of Organic-Inorganic Hybrid Materials and Nanocomposites*; American Scientific: Los Angeles, 2003; Vol. 2.
26. Embs, F. W.; Thomas, E. L.; Wung, C. J.; Prasad, P. N. *Polymer* 1993, 34, 4607.
27. Wang, Y.; Huang, J. S. *J Appl Polym Sci* 1996, 60, 1779.
28. Ettlinger, M.; Ladwig, T.; Weise, A. *Prog Org Coat* 2000, 40, 31.
29. Dong, W. C.; Byoung, C. K. *Polym Adv Technol* 2005, 16, 846.
30. Koti Reddy, C.; Yugandhar, R. L.; Srinivas, P. V. S. S.; Shanthan Rao, P.; Shekharam, T.; Shailaja, D. *J Appl Polym Sci* 2011, 122, 1807.